THE JOURNAL OF PHYSICAL CHEMISTRY B

Article

pubs.acs.org/JPCB

Driving β-Strands into Fibrils

Zhaoqian Su and Cristiano L. Dias*

Physics Department, New Jersey Institute of Technology, Newark, New Jersey 07102-1982, United States

Supporting Information

ABSTRACT: In this work we study contributions of mainchain and side chain atoms to fibrillization of polyalanine peptides using all-atom molecular dynamics simulations. We show that the total number of hydrogen bonds in the system does not change significantly during aggregation. This emerges from a compensatory mechanism where the formation of one interpeptide hydrogen bond requires rupture of two peptide−water bonds, leading to the formation of one extra water−water bond. Since hydrogen bonds are mostly electrostatic in nature, this mechanism implies that electrostatic energies related to these bonds are not minimized during fibril formation. Therefore, hydrogen bonds do not drive fibrillization in all-atom models. Nevertheless, they play an important role in this process since aggregation without the formation of interpeptide hydrogen bonds accounts for a prohibitively large electrostatic penalty (∼9.4 kJ/mol). Our work also highlights the importance of using accurate models to describe chemical bonds since Lennard-Jones and electrostatic contributions of different chemical groups of the protein and solvent are 1 order of magnitude larger than the overall enthalpy of the system. Thus, small errors in modeling these interactions can produce large errors in the total enthalpy of the system.

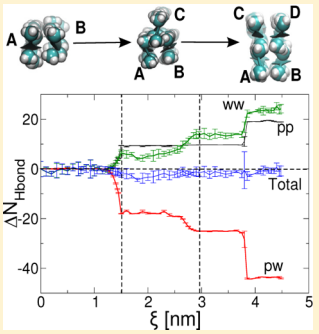

INTRODUCTION

The hierarchical organization of building blocks into complex supra-structures is a recurrent theme in biology. At the molecular level, α-helices and β-strands are building units that pack into globular shapes forming the native state of proteins.[1,2] The length of these units and their packing topology accounts for the diversity of known protein folds. The formation of protein cross-β or fibril structures is a simpler case of hierarchical organization in which β-strand building blocks are identical.[3−6] These conformations have been subjected to numerous studies, as they are linked to diseases like Alzheimer's and Parkinson's.[7] However, despite these studies, it is still not clear what forces are driving peptides into β-sheets and fibrils, and how they differ from the ones driving residues into globular proteins.[8] This is of fundamental importance to understand the pathology of diseases, and it is the focus of the present work.

Under appropriate experimental conditions, X-ray patterns corresponding to cross-β structures have been identified for proteins with seemingly unrelated amino acid sequences.[9−12] This ubiquity suggests that backbone properties (which are common to all proteins) could be responsible for fibrils.[9] Accordingly, energetic models of the Protein Data Bank (PDB) have shown that the free-energy landscape for misfolding is dominated by interactions involving backbone atoms.[13,14] In this framework, the role of side chains is to modulate the propensity of fibril formation.[15] In particular, experiments have shown that mutations accounting for an increase in the concentration of nonpolar residues in the fibril core have a higher fibrillization rate,[16−18] while an increase in the net peptide charge has the opposite effect.[19] This has led to the formulation of the amyloid self-organization principle according to which fibril stability is enhanced by maximizing the number of hydrophobic and favorable electrostatic interactions (including salt bridges and hydrogen bonds).[20−22] Despite these insights, the question of how backbone and side chain atoms contribute to fibrillization is still open.

Thermodynamics provides a quantitative framework to study the forces driving conformational changes in proteins.[23] These phenomena are often described by a two-state reaction equation with an equilibrium constant, K, that can be measured and used to compute differences in Gibbs free energy, $\Delta G = -RT\ \ln(K)$.[24,25] These free energy differences result usually from the sum of large opposing terms. For example, in protein folding at ambient conditions the entropic energy $(-T\Delta S)$ favors the unfolded state while enthalpy (ΔH) favors the native state—each term contributing ∼100−200 kcal/mol and resulting in $\Delta G \sim 10$ kcal/mol.[24,26,27] Main contributions to $-T\Delta S$ come from mainchain $(-T\Delta S_{\text{mainchain}})$ and water molecules around the protein $(-T\Delta S_{\text{water}})$, which favor, respectively, unfolded and native states. ΔH emerges from changes in energy due to covalent-bonds (ΔH_{CB}) and noncovalent-bonds (ΔH_{NCB}). Thus,

$$\Delta G = -T\Delta S_{\text{mainchain}} - T\Delta S_{\text{water}} + \Delta H_{\text{CB}} + \Delta H_{\text{NCB}} \quad (1)$$

The four terms in the right-hand-side of eq 1 are not directly accessible experimentally. This has led to controversies in molecular interpretations of measured $-T\Delta S$ and ΔH. For example, in protein folding at ambient conditions, the entropic energy of water molecules around nonpolar groups, which gives rise to hydrophobic interactions,[28] is believed to be the main force driving protein folding.[29−31] However, $-T\Delta S$, which is the entropic quantity that can be measured experimentally,

Received: May 15, 2014
Revised: August 22, 2014
Published: August 26, 2014

appears unfavorable to the folded state. This is because it is dominated by $-T\Delta S_{mainchain}$. Thus, studies aiming to describe protein folding have shifted back and forth between side chain and backbone centered views.[32−34]

In protein folding, the importance of hydrophobic interactions can be inferred from the positive curvature of ΔG with respect to temperature[24,29,35−37] which is characteristic of nonpolar solvation[38] and accounts for heat and cold denaturations of proteins.[39−45] Also, the diversity of native folds can only be encoded in the amino acid sequence, suggesting that side chain properties and, in particular, the burial of nonpolar side chains in the dry protein core have to be responsible for folding. Currently, it is still a question of debate how intra- and interpeptide hydrogen bonds contribute to secondary-structure formation.[46] It is being argued that hydrogen bonding are stabilizing[47−49] and destabilizing.[29,30,50,51] This question is of fundamental importance to understand fibril formation as interpeptide hydrogen bonds are maximized in these structures.

Here we study fibril formation using extended polyalanine peptides as unit blocks for aggregation and an umbrella sampling protocol to compute free energies to form peptide dimer, trimer, and tetramer. The latter can be considered the smallest repeating unit of a fibril. We find that Lennard-Jones and electrostatic energies of chemical groups in the protein and solvent are 1 order of magnitude larger than the overall enthalpy of the system. Thus, small errors in modeling these interactions can account for large errors in the total enthalpy of the system, highlighting the need for accurate models. We show that the total average number of hydrogen bonds in the system does not change during aggregation as the result of a compensatory mechanism where the formation of one interpeptide hydrogen bond accounts for the rupture of two peptide−water bonds and the release of water molecules from the neighborhood of the peptide leading to the formation of one extra water−water bond.[29,52−55] A consequence of this compensation is that electrostatic energies related to hydrogen bonds are not minimized during fibril formation. Thus, hydrogen bonds do not drive fibril formation. However, we argue that interpeptide hydrogen bonds play an important role in fibril formation since aggregation without the formation of these bonds is energetically prohibitive. Both mainchain and side chain atoms contribute actively to minimize Lennard-Jones interactions during fibril formation. This knowledge of how different chemical groups of the protein contribute to minimize the energy of the system is of fundamental importance to develop strategies to inhibit fibrilization related to diseases and to develop better coarse-grain models of proteins.

METHODOLOGY

The system studied in this work consists of up to four poly alanine peptides, i.e., ALA_{10}, immersed in a periodic box containing 5500 TIP3P water molecules (0.03 M peptide). Polyalanine peptides have been shown experimentally to aggregate and to form fibrils at conditions of 10 μM peptide, pH 7, 0.1 M salts at 25 °C[56] (see also ref 10). In our simulations, peptides are made "infinite" through the use of periodic boundary conditions by attaching the carbonyl-group of residue 1 to the amine-group of residue 10 in the z-direction. The use of "infinite" peptides eliminates effects from chain ends, causing all residues to be equivalent and to resemble amino acids in the middle of a β-strand. A pressure of 38 bar is applied along the z-direction to keep the box from collapsing. The magnitude of this pressure is chosen to ensure an average peptide length of ∼3.5 nm. Therefore, peptides are stretched in our simulations. Notice that the main energetic term opposing aggregation in eq 1 is the reduction in the entropy of the mainchain. This "dissociation" force is not taken into account in our simulations since mainchain entropies of stretched peptides are essentially the same in all states, implying that $-T\Delta S_{mainchain} = 0$ in eq 1. Our simulation setup is designed to describe "aggregations" forces, i.e., changes in the enthalpy of peptide/water and entropy of water (ΔH_{CB}, ΔH_{NCB}, and $-\Delta S_{water}$ in eq 1) when solvated amino acids are brought to interact with each other.

A pressure of 1 atm is applied along the x and y directions to account for water density at ambient pressure. Simulations are carried out using GROMACS and the Amber99-sd-ildn force field.[57] Temperature (298 K) and pressure are controlled using the v-rescale thermostat (τ_T = 1 ps) and the Parrinello−Rahman barostat (τ_P = 1 ps), respectively. A time step of 2 fs is used, and the neighbor list is updated every 10 steps. Electrostatics is treated using the smooth particle mesh Ewald method with a grid spacing of 0.13 nm and a 1.3 nm real-space cutoff.[58]

To determine the free-energy landscape of peptide tetramer formation, we perform three sets of simulations containing two, three, and four peptides, respectively. In the first set, peptides are arranged in an antiparallel orientation and an umbrella sampling protocol is used to sample the space given by the distance between centers-of-mass of peptides (ξ_2 in Figure 1a)

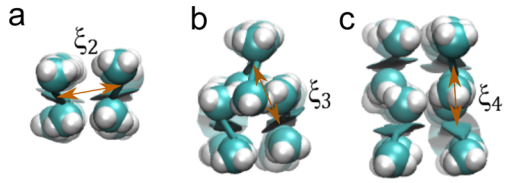

Figure 1. Schematic representation of the reaction coordinate used to study the formation of peptide dimer (a), trimer (b), and tetramer (c).

in the range 0.4 to 2.0 nm. Different windows in which peptides are restrained by a spring that has a constant of 5000 kJ mol^{-1} nm^{-2} are simulated. Equilibrium distances of springs in neighboring windows differ in steps of 0.05 nm. Each window is simulated for 100 ns and the potential of mean force (PMF) to form a dimer is computed using the weighted histogram analysis method (WHAM).[59] In coarse-grained simulations fibrillization was found to start with the formation of antiparallel structures follow by a transition to parallel conformations after enough peptides are added to β-sheets.[60−62] This suggests that parallel β-structures are less stable than antiparallel ones when sheets are formed by a small number of peptides while the opposite is expected for large sheets. For polyvaline, the number of peptides required to stabilize parallel β-sheet was found to be 14.[60] While the scope of the present work is not to study this transition, we show as Supporting Information (SI) that parallel β-sheets involving two peptides are indeed less stable than antiparallel ones.

To perform the second set of simulations, a peptide is added to the simulation box of the dimer. In these simulations, a spring is used to restrain centers-of-mass of the dimer at a distance corresponding to the minimum of its PMF. Umbrella sampling simulations are repeated for this new system to sample the distance between centers-of-mass of a reference

dx.doi.org/10.1021/jp504798s | J. Phys. Chem. B 2014, 118, 10830−10836

peptide in the dimer and the additional chain (ξ_3 in Figure 1*b*). Configurations from these simulations are used to compute the PMF of trimer formation using WHAM. At last, the trimer is restrain to the configuration corresponding to the minimium in its PMF using two springs connecting a reference peptide to the other two chains. A peptide is added to the simulation box which now comprises two sets of antiparallel peptides. Umbrella sampling simulations are performed using the distance between the reference peptide in the trimer and the added chain as the new reaction coordinate (ξ_4 in Figure 1*c*). The PMF to form a tetramer is computed using WHAM.

To define hydrogen bonds we employ a commonly used geometrical definition in which these bonds are formed when the distance between hydrogen (H) donor (D) and acceptor (A) is smaller than 0.4 nm and the angle H-D-A is smaller than 30°. In the calculation of quantities involving solute−solvent and solvent−solvent atoms, all solvent (water) molecules were taken into account. In the calculation of spatial distribution functions of water (see Figure 4) the simulation box was divided in bins of length 0.02 nm. Spatial distribution functions are given in units of the ratio of the density of water in the simulation and the density of water of an ideal fluid for each bin.

RESULTS

In Figure 2a we show PMF(s) of peptide dimer, trimer, and tetramer. These three PMF(s) are computed separately as described in the Methodology section and the continuous reaction coordinate ξ is obtained by concatenating inverted order parameters of peptide dimer ($\xi_2^{new} = 2.0 - \xi_2$), trimer ($\xi_3^{new} = 2.0 - \xi_3$), and tetramer ($\xi_4^{new} = 2.0 - \xi_4$). In this procedure, the PMF of the peptide trimer at $\xi_3^{new} = 0.0$ is shifted to match the minimum in the PMF of the peptide dimer. Similarly for the tetramer: its PMF at $\xi_4^{new} = 0.0$ is shifted to match the free-energy minimum of the trimeric system. This concatenation procedure describes the assembly of fibrils through monomer addition[63,64] where peptide dimer is formed first followed by docking of a third peptide and subsequent tetramer formation.

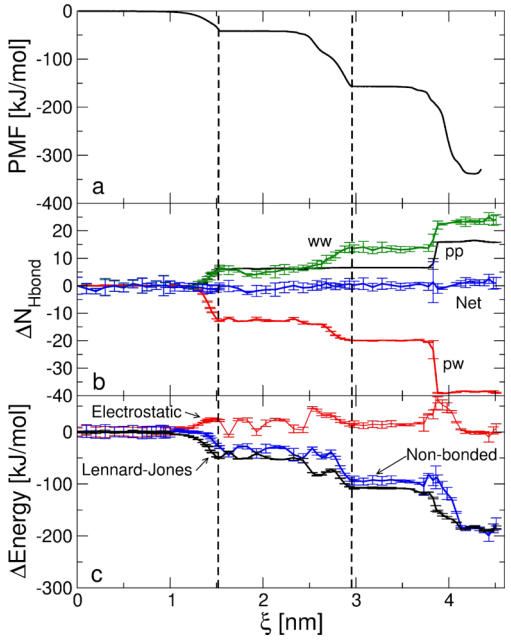

Figure 2. PMF (a), number of hydrogen bonds (b), and potential energy (c) to assemble β-strands in a hierarchical process. These quantities were computed with respect to their values at non-interacting peptide conformations ($\xi = 0$). Number of hydrogen bonds was divided into contributions from peptide−peptide (pp), water−water (ww), and peptide−water (pw). The net number of hydrogen bonds is also shown. The potential energy was divided into electrostatic and van der Waals contributions. Dashed lines separate simulations of dimer (left), trimer (middle), and tetramer (right). Error bars were estimated from block averages by dividing the simulation in five blocks.

In Figure 2*b* we show how numbers of hydrogen bonds in the system change during peptide dimer, trimer, and tetramer formation. The number of hydrogen bonds for isolated peptides is used as a reference, i.e., $N_{Hbond}(\xi = 0) \equiv 0$. For all values of ξ, the total (or net) number of hydrogen bonds does not change significantly. A similar behavior was reported recently for β-hairpin formation of GB1 peptide[65] and β-sheet formation of model peptides made of glycine, alanine, valine, and leucine residues.[66] To understand this result in more detail, we decompose the total number of hydrogen bonds into contributions from peptide−peptide, peptide−water, and water−water bonds. We observe an almost perfect compensatory mechanism[29,52−55] where the formation of one peptide−peptide hydrogen bond is preceded by the rupture of two peptide-water bonds accounting for water release into the bulk and the formation of one additional water−water bond. Notice that during peptide trimer formation (at $\xi \sim 2.8$ nm) the third peptide docks onto the dimer (i.e., β-sheet) without forming interpeptide hydrogen bonds (see Figure 1). This process involves displacement of water molecules from the space between side chains in the β-sheet (see "HB" configuration in Figure 4*a*) to the bulk during docking. In this case, rupture of peptide−water hydrogen bonds during docking of the third peptide is compensated by newly formed water−water bonds. The generality of the observed hydrogen bond compensation for peptides with different amino acid sequences and situations might be due to the small size and polarity of water which can penetrates small cavities to saturate nonsatisfied hydrogen bonds.[67,68]

In all-atom models, hydrogen bonds emerge from electrostatic interactions involving X−H···Y chemical groups, where X and Y are electronegative atoms and H is hydrogen. Thus, if hydrogen bonds are a main force driving aggregation, the electrostatic energy is expected to correlate with the PMF, i.e., it should decrease whenever the PMF become a minimum. In Figure 2c we show the dependence of the electrostatic energy of the system on the reaction coordinate ξ. It does not correlate with the PMF being mostly indifferent to tetramer formation. In contrast, the energy due to Lennard-Jones interactions is favorable to peptide aggregation. As a result, the sum of Lennard-Jones and electrostatic energy, i.e., nonbonded interactions, is favorable to aggregation.

Figure 3 quantifies contributions of different chemical groups to changes in electrostatic and Lennard-Jones energies. Panel a shows a compensatory mechanism for electrostatic interactions where unfavorable mainchain−water interactions are balanced by favorable water−water and mainchain−mainchain interactions. Since nitrogen and oxygen are mainchain atoms contributing the most to the peptide's electrostatic energy, the observed compensatory mechanism for the electrostatic energy can be mapped to the formation of one interpeptide hydrogen bond which requires breakage of two peptide−water hydrogen

dx.doi.org/10.1021/jp504798s | J. Phys. Chem. B 2014, 118, 10830−10836

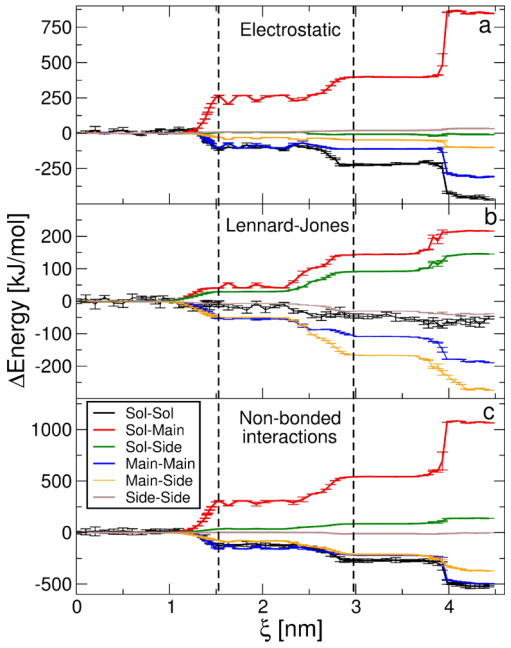

Figure 3. Contribution of different chemical groups of the protein and solvent to tetramer formation. Electrostatic (a), Lennard-Jones (b), and nonbonded-interactions (c) are decomposed into solvent−solvent (black), solvent-mainchain (red), solvent-side chain (green), mainchain−mainchain (blue), mainchain−side chain (orange), and side chain−side chain (brown) contributions.

bonds and subsequent formation of one water−water hydrogen bond. Moreover, the total change in electrostatic energy emerging from these contributions is approximately zero, as shown in Figure 2c. Hence, it is not expected to drive aggregation. However, a hypothetical process in which mainchain NH− and CO− groups are buried away from water without forming inter- or intrapeptide hydrogen bonds would increase the electrostatic energy by a prohibitive large amount, i.e., $E^{elect}_{Sol-Main} + E^{elect}_{Sol-Sol} \sim 9.4$ kJ/mol/residue. This suggests that a main role of inter- and/or intrapeptide hydrogen bonds is to penalize structures for which the overall number of hydrogen bonds in the system is not optimized.

Notice that in implicit water models the formation of mainchain hydrogen bonds is taken into account by a decrease in the energy of the system.[69] This favors peptide conformations with optimized secondary structures. This approach was successful in predicting the structure of various nonamyloid[70−74] and amyloid[75,76] peptides. However, this description of hydrogen bonds does not mimic the energetics of explicit water simulations as described above. Thus, there is a trade-off between accounting for the entropic contribution of the backbone using implicit water coarse-grained models and describing with greater accuracy noncovalent interactions using all-atom models. A successful strategy could be to combine these two approaches.[77]

Figure 3b shows how burial of side chain and mainchain atoms away from water during aggregation affects Lennard-Jones interactions. In this process, water molecules are transferred to the bulk, accounting for a modest decrease in Lennard-Jones energy. This change is comparable to the reduction in Lennard-Jones energy due to side chain-side chain interactions. Main contributions to changes in Lennard-Jones energy are due to water−mainchain, water−side chain, mainchain−mainchain, and mainchain−side chain interactions. Breaking bonds between water and peptide atoms, i.e., water−mainchain and water−side chain bonds, accounts for the large increase in Lennard-Jones energy. However, this process is overcompensated by the favorable formations of new bonds between atoms of the peptide, i.e., mainchain−mainchain and mainchain−side chain. This leads to a net Lennard-Jones energy that is favorable to aggregation, as shown in Figure 2c.

Figure 3c shows the sum of Lennard-Jones and electrostatic energies, i.e., nonbonded energies, for interactions between the different chemical groups of the system. The overall nonbonded energy is favorable to aggregation (as displayed in Figure 2c) and Figure 3c shows that it emerges from large contributing terms that have opposite signs. Contributing terms are 1 order of magnitude larger than the overall nonbonded energy. This highlights the importance of using accurate models since small errors in modeling the strength of one bond can produce large errors in the total enthalpy of the system.

In Figure 4 we show the spatial distribution of water around ground states of peptide dimer (panel a), trimer (b), and

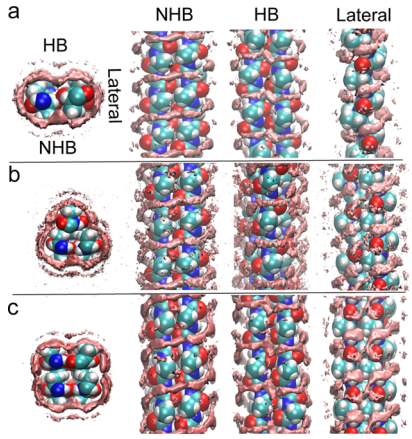

Figure 4. Iso-surface of water distribution around the ground state of dimer (a), trimer (b), and tetramer (c). Columns correspond to cross-sections of the peptide's axis, non-hydrogen-bonded face (NHB), hydrogen-bonded face (HB), and lateral view. Isovalues of dimer, trimer, and tetramer are 5.04278, 5.04278, and 10.5715, respectively.

tetramer (c). The first column corresponds to cross sections of the peptide's main axis. In an antiparallel β-sheet, residues along a strand can either be hydrogen-bonded to the neighboring strand or non-hydrogen-bonded.[78,79] Side chains of hydrogen-bonded residues all face the same direction, which is called the hydrogen-bonded face (HB) of the β-sheet. Similarly defined is the non-hydrogen-bonded face (NHB). A detailed analysis of water distribution around a β-sheet for different nonpolar amino acids was reported recently.[80] It showed that water distribution is different at HB and NHB faces. This result was particularly striking for leucine and valine residues. For alanine, polar groups of the mainchain are more exposed to water at the NHB face compared to HB. Thus, water molecules were shown to penetrate deeper in the space between side chains at the NHB face. This result is visible in the cross-section view of dimers and tetramers where iso-surfaces are more pronounced and penetrate deeper between side chains at the NHB face. At the HB face, distributions of water in addition of being perpendicular to the axis of the peptide also have a parallel component that enhances electrostatic interactions between water and polar groups of the mainchain that are partially buried between C_α atoms. The lateral view (last column in

dx.doi.org/10.1021/jp504798s | J. Phys. Chem. B 2014, 118, 10830−10836

Figure 4) shows a more pronounced distribution of water facing NH− groups of the mainchain compared to CO− groups. This result was studied in detail in ref 80, and it was related to the hydrogen-receiver nature of the CO− group, which allows hydrogen-bonding with water with a greater angular freedom.

CONCLUSION

In summary, to investigate the energetics of fibril formation, we performed extensive molecular dynamics simulations of polyalanine in water. To understand which chemical groups of the peptide favor fibril formation, we decomposed nonbonded interactions into contributions from mainchain and side chain atoms. We show that changes in the energy of the system due to mainchain atoms play a major role in this process. We used a geometrical definition to compute the number of hydrogen bonds in the system. We show that, due to a compensatory mechanism, the total number of hydrogen bonds in the system does not change significantly during fibrillization.[29,52,54,55] Furthermore, main changes in the electrostatic energy of the system are related to hydrogen bonds and, as a result of the compensatory mechanism, it does not decrease during fibrillization. Thus, while fibril formation accounts for an increase in the number interpeptide hydrogen bonds, there is no apparent energy gain in the formation of these bonds. This leads to the question of what is the energetic role of interpeptide hydrogen bonds?[46]

We argue that peptide aggregation without the formation of interpeptide hydrogen bonds produces a large electrostatic penalty. Thus, in all-atom simulations, secondary structures do not form to minimize energetic terms associated with hydrogen bonds but to avoid the energetic penalty of having nonsatisfied polar groups pointing toward the dry core of the protein. This implies that disordered configurations with polar groups exposed to water and secondary-structure configurations might not be very different with respect to the energy of hydrogen bonds. Therefore, the main role of hydrogen bonds is to reduce the number of peptide conformations and, in particular, the number of compact peptide structures. This result could have important implications for the development of coarse-grained models.

Moreover, if we assume that energies to form side chain−side chain and mainchain−mainchain hydrogen bonds are similar then our results suggest that burial of nonpolar side chains in the protein core without the formations of hydrogen bonds could be subjected to large penalties. Thus, conformational changes of proteins after the formation of a dry core would involve little change in the number of both side chain and backbone hydrogen bonds since this requires overcoming large energy barriers. This is consistent with reported results from coarse grained simulations in which transitions between β-barrel structures and fibrils for the polar NHVTLSQ peptide occurred with little variation in the number of hydrogen bonds.[81] In addition, the penalty of having nonsaturated hydrogen bonds in the protein core could be responsible for faster fibrillization rates of polar sequences compared to nonpolar ones,[82] since the formation of side chain hydrogen bonds would occur promptly after the creation of a dry core in the case of polar sequences, while a larger (and more frustrated) phase space has to be sampled before in-registry fibrils can form in nonpolar peptides. In the case of transmembrane proteins, it has been reported that hydrogen bonds between polar side chains and the backbone play an important role in the dynamics and stability of α-helical structures.[83] This is also consistent with our results that associate an energetic penalty to polar side chains exposed to membranes that can, however, be minimized through side chain-mainchain hydrogen bonding.

Despite these conceptual and quantitative contributions, limitations of the current work should also be noted. While all-atom models have been optimized over the years to account for folding of several proteins,[84,85] there are still uncertainties regarding force-field parameters. In particular, all-atom models do not account for context-dependent interactions, whereas experiments suggest that the strength of hydrogen bonds could be dependent on the environment.[47,86−89] Moreover, the setup used in this work only considers stretched peptide structures, which is a geometry that facilitates the observed compensatory mechanism for hydrogen bonds. In contrast, when peptides are not interacting, they can assume conformations for which the total number of hydrogen bonds in the system is not optimized. While results on the GB1 model peptide show that the compensatory mechanism is also valid for unconstrained structures,[65] this requires further investigation.

ASSOCIATED CONTENT

Supporting Information

Comparison of PMFs for the interaction of two parallel and two anti-parallel polyalanine peptides, structure of two parallel polyalanine peptides at ξ = 0.47 nm, and dependence of the number of hydrogen bonds on the distance between the centers-of-mass of peptides. This material is available free of charge via the Internet at http://pubs.acs.org.

AUTHOR INFORMATION

Corresponding Author

*E-mail: cld@njit.edu.

Notes

The authors declare no competing financial interest.

ACKNOWLEDGMENTS

This work was made possible by NJIT start-up funds and computational resources available through Compute Canada and High Performance Computing at NJIT. C.L.D. would also like to thank Robert Baldwin for insightful comments on the manuscript.

REFERENCES

(1) Pauling, L.; Corey, R. B. Configurations of Polypeptide Chains With Favored Orientations Around Single Bonds. *Proc. Natl. Acad. Sci. U. S. A.* **1951**, *37*, 729−740.

(2) Pauling, L.; Corey, R. B. Two New Pleated Sheets. *Proc. Natl. Acad. Sci. U. S. A.* **1951**, *37*, 729.

(3) Eanes, E. D.; Glenner, G. G. X-ray Diffraction Studies on Amyloid Filaments. *J. Histochem. Cytochem.* **1968**, *16*, 673.

(4) Geddes, A.; Parker, K.; Atkins, E.; Beighton, E. Cross-β Conformation in Proteins. *J. Mol. Biol.* **1968**, *32*, 343.

(5) Nelson, R.; Sawaya, M. R.; Balbirnie, M.; Madsen, A. O.; Riekel, C.; Grothe, R.; Eisenberg, D. Structure of the Cross-β Spine of Amyloid-Like Fibrils. *Nature* **2005**, *435*, 773.

(6) Perczel, A.; Hudáky, P.; Pálfi, V. K. Dead-End Street of Protein Folding: Thermodynamic Rationale of Amyloid Fibril Formation. *J. Am. Chem. Soc.* **2007**, *129*, 14959.

(7) Dobson, C. M. Protein Folding and Misfolding. *Nature* **2003**, *426*, 884.

(8) Schmit, J.; Ghosh, K.; Dill, K. A. What Drives Amyloid Molecules to Assemble into Oligomers and Fibrils? *Biophys. J.* **2011**, *100*, 450.

(9) Fändrich, M.; Fletcher, M. A.; Dobson, C. M. Amyloid Fibrils from Muscle Myoglobin. *Nature* **2001**, *410*, 165.
(10) Fändrich, M.; Dobson, M. Christopher The Behaviour of Polyamino Acids Reveals an Inverse Side Chain Effect in Amyloid Structure Formation. *EMBO J.* **2002**, *21*, 5682.
(11) Sawaya, M. R.; Sambashivan, S.; Nelson, R.; Ivanova, M. I.; Sievers, S. A.; Apostol, M. I.; Thompson, M. J.; Balbirnie, M.; Wiltzius, J. J. W.; McFarlane, M. A. .; Heather, T.; Riekel, C.; Eisenberg, D. Atomic Structures of Amyloid Cross-Beta Spines Reveal Varied Steric Zippers. *Nature* **2007**, *447*, 453.
(12) Tycko, R. Insights into the Amyloid Folding Problem from Solid-State NMR. *Biochemistry* **2003**, *42*, 3151.
(13) Fitzpatrick, A. W.; Knowles, T. P. J.; Waudby, C. A.; Vendruscolo, M.; Dobson, C. M. Inversion of the Balance between Hydrophobic and Hydrogen Bonding Interactions in Protein Folding and Aggregation. *PLoS Comput. Biol.* **2011**, *7*, e10002169.
(14) Cheon, M.; Chang, I.; Mohanty, S.; Luheshi, L. M.; Dobson, C. M.; Vendruscolo, M.; Favrin, G. Structural Reorganisation and Potential Toxicity of Oligomeric Species Formed during the Assembly of Amyloid Fibrils. *PLoS Comput. Biol.* **2007**, *3*, e173.
(15) Chiti, F.; Dobson, C. M. Protein Misfolding, Functional Amyloid, and Human Disease. *Annu. Rev. Biochem.* **2006**, *75*, 333.
(16) Otzen, D. E.; Kristensen, O.; Oliveberg, M. Designed Protein Tetramer Zipped Together with a Hydrophobic Alzheimer Homology: A Structural Clue to Amyloid Assembly. *Proc. Natl. Acad. Sci. U.S.A.* **2000**, *97*, 9907.
(17) de la Paz, M. L.; de Mori, G. M.; Serrano, L.; Colombo, G. Sequence Dependence of Amyloid Fibril Formation: Insights from Molecular Dynamics Simulations. *J. Mol. Biol.* **2005**, *349*, 583.
(18) Gazit, E. A Possible Role for π-Stacking in the Self-Assembly of Amyloid Fibrils. *FASEB J.* **2002**, *16*, 77.
(19) Chiti, F.; Calamai, M.; Taddei, N.; Stefani, M.; Ramponi, G.; Dobson, C. M. Studies of the Aggregation of Mutant Proteins in Vitro Provide Insights into the Genetics of Amyloid Diseases. *Proc. Natl. Acad. Sci. U. S. A.* **2002**, *99*, 16419.
(20) Thirumalai, D.; Reddy, G.; Straub, J. E. Role of Water in Protein Aggregation and Amyloid Polymorphism. *Acc. Chem. Res.* **2012**, *45*, 83.
(21) Tarus, B.; Straub, J. E.; Thirumalai, D. Dynamics of Asp23-Lys28 Salt-Bridge Formation in Aβ_{10-35} Monomers. *J. Am. Chem. Soc.* **2006**, *128*, 16159.
(22) Straub, J. E.; Thirumalai, D. Principles Governing Oligomer Formation in Amyloidogenic Peptides. *Curr. Opin. Struct. Biol.* **2010**, *20*, 187.
(23) Anfinsen, C. B. Principles that Govern the Folding of Protein Chains. *Science* **1973**, *181*, 223.
(24) Privalov, P. L. Cold Denaturation of Protein. *Crit. Rev. Biochem. Mol. Biol.* **1990**, *25*, 281.
(25) Privalov, P. L. Thermodynamics of Protein Folding. *J. Chem. Thermodynamics* **1997**, *29*, 447.
(26) Brandts, J. F. The Thermodynamics of Protein Denaturation. I. The Denaturation of Chymotrypsinogen. *J. Am. Chem. Soc.* **1964**, *86*, 4291.
(27) Brandts, J. F. The Thermodynamics of Protein Denaturation. II. A Model of Reversible Denaturation and Interpretations Regarding the Stability of Chymotrypsinogen. *J. Am. Chem. Soc.* **1964**, *86*, 4302.
(28) Frank, H. S.; Evans, M. W. Free Volume and Entropy in Condensed Systems III. Entropy in Binary Liquid Mixtures; Partial Molal Entropy in Dilute Solutions; Structure and Thermodynamics in Aqueous Electrolytes. *J. Chem. Phys.* **1945**, *13*, 507.
(29) Kauzmann, W. Some Factors in the Interpretation of Protein Denaturation. *Adv. Protein Chem.* **1959**, *14*, 1.
(30) Dill, K. Dominant Forces in Protein Folding. *Biochemistry* **1990**, *29*, 7133.
(31) Li, H.; Tang, C.; Wingreen, N. S. Nature of Driving Force for Protein Folding: A Result From Analyzing the Statistical Potential. *Phys. Rev. Lett.* **1997**, *79*, 765.
(32) Ma, B.; Nussinov, R. Molecular Dynamics Simulations of a β-Hairpin Fragment of Protein G: Balance Between Side-Chain and Backbone Forces. *J. Mol. Biol.* **2000**, *296*, 1091.
(33) Rose, G. D.; Wolfenden, R. Hydrogen Bonding, Hydrophobicity, Packing, and Protein Folding. *Annu. Rev. Biophys. Biomol. Struct.* **1993**, *22*, 381.
(34) Bolen, D. W.; Rose, G. D. Structure and Energetics of the Hydrogen-Bonded Backbone in Protein Folding. *Annu. Rev. Biochem.* **2008**, *77*, 339.
(35) Dias, C. L.; Ala-Nissila, T.; Wong-ekkabut, J.; Vattulainen, I.; Grant, M.; Karttunen, M. The Hydrophobic Effect and Its Role in Cold Denaturation. *Cryobiology* **2010**, *60*, 91.
(36) Baldwin, R. L. Energetics of Protein Folding. *J. Mol. Biol.* **2007**, *371*, 283.
(37) Shimizu, S.; Chan, H. S. Temperature Dependence of Hydrophobic Interactions: A Mean Force Perspective, Effects of Water Density, and Nonadditivity of Thermodynamic Signatures. *J. Chem. Phys.* **2000**, *113*, 4683.
(38) Edsall, J. T. Apparent Molal Heat Capacities of Amino Acids and Other Organic Compounds. *J. Am. Chem. Soc.* **1935**, *54*, 1506–1507.
(39) Rios, P. D. L.; Caldarelli, G. Putting Proteins Back into Water. *Phys. Rev. E* **2000**, *62*, 8449.
(40) Rios, P. D. L.; Caldarelli, G. Cold and Warm Swelling of Hydrophobic Polymers. *Phys. Rev. E* **2001**, *63*, 031802.
(41) Dias, C. L.; Ala-Nissila, T.; Karttunen, M.; Vattulainen, I.; Grant, M. Microscopic Mechanism for Cold Denaturation. *Phys. Rev. Lett.* **2008**, *100*, 118101.
(42) Dias, C. L. Unifying Microscopic Mechanism for Pressure and Cold Denaturations of Proteins. *Phys. Rev. Lett.* **2012**, *109*, 048104.
(43) Privalov, P. L.; Griko, Y. V.; Venyaminov, S. Y. Cold Denaturation of Myoglobin. *J. Mol. Biol.* **1986**, *190*, 487.
(44) Privalov, P. L.; Gill, S. J. The Hydrophobic Effect: A Reappraisal. *Pure Appl. Chem.* **1989**, *61*, 1097.
(45) Dias, C. L.; Chan, H. S. Pressure-Dependence Properties of Elementary Hydrophobic Interactions: Ramifications for Activation Properties of Protein Folding. *J. Phys. Chem. B* **2014**, *118*, 7488.
(46) Baldwin, R. L. In Search of the Energetic Role of Peptide Hydrogen Bonds. *J. Biol. Chem.* **2003**, *278*, 17581.
(47) Gao, J.; Bosco, D. A.; Powers, E. T.; Kelly, J. W. Localized Thermodynamic Coupling Between Hydrogen Bonding and Microenvironment Polarity Substantially Stabilizes Proteins. *Nat. Struct. Mol. Biol.* **2009**, *16*, 684.
(48) Bolen, D. W.; Rose, G. D. Structure and Energetics of the Hydrogen-Bonded Backbone in Protein Folding. *Annu. Rev. Biochem.* **2008**, *77*, 339.
(49) Rose, G. D.; Fleming, P. J.; Banavar, J. R.; Maritan, A. A Backbone-Based Theory of Protein Folding. *Proc. Natl. Acad. Sci. U. S. A.* **2006**, *103*, 16623.
(50) Ma, B.; Nussinov, R. Molecular Dynamics Simulations of Alanine Rich β-Sheet Oligomers: Insight into Amyloid Formation. *Protein Sci.* **2002**, *11*, 2335.
(51) Yang, A.-S.; Honig, B. Free Energy Determinants of Secondary Structure Formation: II. Antiparallel β-Sheets. *J. Mol. Biol.* **1995**, *252*, 366.
(52) Fersht, A. R.; Shi, J.-P.; Knill-Jones, J.; Lowe, D. M.; Wilkinson, A. J.; Blow, D. M.; Brick, P.; Carter, P.; Waye, M. M. Y.; Winter, G. Hydrogen Bonding and Biological Specificity Analysed by Protein Engineering. *Nature* **1985**, *314*, 235.
(53) Fersht, A. R. The Hydrogen Bond in Molecular Recognition. *Trends Biochem. Sci.* **1987**, *12*, 301.
(54) Takeda, T.; Klimov, D. K. Computational Backbone Mutagenesis of Aβ Peptides: Probing the Role of Backbone Hydrogen Bonds in Aggregation. *J. Phys. Chem. B* **2010**, *114*, 4755.
(55) Jorgensen, W. L. Interactions Between Amides in Solution and the Thermodynamics of Weak Binding. *J. Am. Chem. Soc.* **1989**, *111*, 3770.
(56) Bernacki, J. P.; Regina, M. M. Length-Dependent Aggregation of Uninterrupted Polyalanine Peptides. *Biochemistry* **2011**, *50*, 9200.
(57) Lindorff-Larsen, K.; Piana, S.; Palmo, K.; Maragakis, P.; Klepeis, J. L.; Dror, R. O.; Shaw, D. E. Improved Side-Chain Torsion Potentials

for the Amber ff99SB Protein Force Field. *Proteins: Struct., Funct., Bioinf.* **2010**, *78*, 1950−1958.
(58) Bjelkmar, P.; Larsson, P.; Cuendet, M. A.; Hess, B.; Lindahl, E. Implementation of the CHARMM Force Field in GROMACS: Analysis of Protein Stability Effects from Correction Maps, Virtual Interaction Sites, and Water Models. *J. Chem. Theory Comput.* **2010**, *6*, 459.
(59) Hub, J. S.; de Groot, B. L.; van der Spoel, D. g_wham—A Free Weighted Histogram Analysis Implementation Including Robust Error and Autocorrelation Estimates. *J. Chem. Theory Comput.* **2010**, *6*, 3713.
(60) Baftizadeh, F.; Biarnes, X.; Pietrucci, F.; Affinito, F.; Laio, A. Multidimensional View of Amyloid Fibril Nucleation in Atomistic Detail. *J. Am. Chem. Soc.* **2012**, *134*, 3886.
(61) Baftizadeh, F.; Pietrucci, F.; Biarnés, X.; Laio, A. Nucleation Process of a Fibril Precursor in the C-Terminal Segment of Amyloid-β. *Phys. Rev. Lett.* **2013**, *110*, 168103.
(62) Nguyen, P.; Derreumaux, P. Understanding Amyloid Fibril Nucleation and Aβ Oligomer/Drug Interactions from Computer Simulations. *Acc. Chem. Res.* **2014**, *47*, 603.
(63) Collins, S.; Douglass, A.; Vale, R.; Weissman, J. Mechanism of Prion Propagation: Amyloid Growth Occurs by Monomer Addition. *PLoS Biol.* **2004**, *2*, e321.
(64) Hills, R. D., Jr.; Brooks, C. L., III. Hydrophobic Cooperativity as a Mechanism for Amyloid Nucleation. *J. Mol. Biol.* **2007**, *368*, 894.
(65) Narayanan, C.; Dias, C. L. Exploring the Free Energy Landscape of a Model β-Hairpin Peptide and Its Isoform. *Proteins: Struct., Funct., Bioinf.* **2014**, DOI: 10.1002/prot.24601.
(66) Narayanan, C.; Dias, C. L. Hydrophobic Interactions and Hydrogen Bonds in β-Sheet Formation. *J. Chem. Phys.* **2013**, *139*, 115103.
(67) Chandler, D. Hydrophobicity: Two Faces of Water. *Nature* **2002**, *417*, 491.
(68) Chandler, D. Interfaces and the Driving Force of Hydrophobic Assembly. *Nature* **2005**, *437*, 640.
(69) Sterpone, F.; Nguyen, P. H.; Kalimeri, M.; Derreumaux, P. Importance of the Ion-Pair Interactions in the OPEP Coarse-Grained Force Field: Parametrization and Validation. *J. Chem. Theory Comput.* **2013**, *9*, 4574.
(70) Wei, G.; Mousseau, N.; Derreumaux, P. Sampling the Self-Assembly Pathways of KFFE Hexamers. *Biophys. J.* **2004**, *87*, 3648.
(71) Chen, W.; Mousseau, N.; Derreumaux, P. The Conformations of the Amyloid-β (21−30) Fragment can be Described by Three Families in Solution. *J. Chem. Phys.* **2006**, *125*, 084911.
(72) Maupetit, J.; Derreumaux, P.; Tufféry, P. A Fast Method for Large-Scale De Novo Peptide and Miniprotein Structure Prediction. *J. Comput. Chem.* **2010**, *31*, 726.
(73) Maupetit, J.; Derreumaux, P.; Tufféry, P. PEP-FOLD: An Online Resource for De Novo Peptide Structure Prediction. *Nucleic Acids Res.* **2009**, *37*, W498.
(74) Santini, S.; Wei, G.; Mousseau, N.; Derreumaux, P. Pathway Complexity of Alzheimer's β-Amyloid Aβ_{16-22} Peptide Assembly. *Structure* **2004**, *12*, 1245.
(75) Chebaro, Y.; Jiang, P.; Zang, T.; Mu, Y.; Nguyen, P. H.; Mousseau, N.; Derreumaux, P. Structures of Aβ17−42 Trimers in Isolation and with Five Small-Molecule Drugs Using a Hierarchical Computational Procedure. *J. Phys. Chem. B* **2012**, *116*, 84.
(76) Ding, F.; LaRocque, J. J.; Dokholyan, N. V. Direct Observation of Protein Folding, Aggregation, and a Prion-like Conformational Conversion. *J. Biol. Chem.* **2005**, *280*, 40235.
(77) Nasica-Labouze, J.; Meli, M.; Derreumaux, P.; Colombo, G.; Mousseau, N. A Multiscale Approach to Characterize the Early Aggregation Steps of the Amyloid-Forming Peptide GNNQQNY from the Yeast Prion Sup-35. *PLoS Comput. Biol.* **2011**, *7*, e1002051.
(78) Cheng, P.-N.; Pham, J. D.; Nowick, J. S. The Supramolecular Chemistry of β-Sheets. *J. Am. Chem. Soc.* **2013**, *135*, 5477.
(79) Hutchinson, E. G.; Sessions, R. B.; Thornton, J. M.; Woolfson, D. N. Determinants of Strand Register in Antiparallel β-Sheets of Proteins. *Protein Sci.* **1998**, *7*, 2287.
(80) Urbic, T.; Dias, C. Hydration of Non-Polar Anti-Parallel Beta-Sheets. *J. Chem. Phys.* **2014**, *140*, 165101.
(81) Song, W.; Wei, G.; Mousseau, N.; Derreumaux, P. Self-Assembly of the β2-Microglobulin NHVTLSQ Peptide Using a Coarse-Grained Protein Model Reveals a β-Barrel Species. *J. Phys. Chem. B* **2008**, *112*, 4410.
(82) Lu, Y.; Derreumaux, P.; Guo, Z.; Mousseau, N.; Wei, G. Thermodynamics and Dynamics of Amyloid Peptide Oligomerization are Sequence Dependent. *Proteins: Struct., Funct., Bioinf.* **2009**, *75*, 954.
(83) Scharnagl, C.; Pester, O.; Hornburg, P.; Hornburg, D.; Götz, A.; Langosch, D. Side-Chain to Main-Chain Hydrogen Bonding Controls the Intrinsic Backbone Dynamics of the Amyloid Precursor Protein Transmembrane Helix. *Biophys. J.* **2014**, *106*, 1318.
(84) Lindorff-Larsen, K.; Piana, S.; Dror, R. O.; Shaw, D. E. How Fast-Folding Proteins Fold. *Science* **2011**, *334*, 6055.
(85) Shaw, D. E.; Maragakis, P.; Lindorff-Larsen, K.; Piana, S.; Dror, R. O.; Eastwood, M. P.; Bank, J. A.; Jumper, J. M.; Salmon, J. K.; Shan, Y.; Wriggers, W. Atomic-Level Characterization of the Structural Dynamics of Proteins. *Science* **2010**, *330*, 60002.
(86) Deechongkit, S.; Nguyen, H.; Powers, E. T.; Dawson, P. E.; Gruebele, M.; Kelly, J. W. Context-Dependent Contributions of Backbone Hydrogen Bonding to β-Sheet Folding Energetics. *Nature* **2004**, *430*, 101.
(87) Deechongkit, S.; Dawson, P. E.; Kelly, J. W. Toward Assessing the Position-Dependent Contributions of Backbone Hydrogen Bonding to β-Sheet Folding Thermodynamics Employing Amide-to-Ester Perturbations. *J. Am. Chem. Soc.* **2004**, *126*, 16762.
(88) Ji, C. G.; Zhang, J. Z. H. Quantifying the Stabilizing Energy of the Intraprotein Hydrogen Bond Due to Local Mutation. *J. Phys. Chem. B* **2011**, *115*, 12230.
(89) Ji, C. G.; Xiao, X.; Zhang, J. Z. H. Studying the Effect of Site-Specific Hydrophobicity and Polarization on Hydrogen Bond Energy of Protein Using a Polarizable Method. *J. Chem. Theory Comput.* **2012**, *8*, 2157−2164.